Direct P-Wave Seismic Noise Interferometry for Groundwater Monitoring: A Modelling Study

Aguzzoli, A.; Draganov, D.S.; Arosio, D.

DIRECT P-WAVE SEISMIC NOISE INTERFEROMETRY FOR GROUNDWATER MONITORING: A MODELLING STUDY

A. Aguzzoli[1], D. Draganov[2], D. Arosio[1]

[1] Università degli Studi di Modena e Reggio Emilia; [2] Delft University of Technology

Summary

In this study, we monitor the depth variation of an unconfined aquifer by applying seismic noise interferometry to synthetic data modelled with a 2D finite-difference software. We consider two models with the same subsurface geological structure, but with different water table levels representing two monitoring periods. The receivers are placed at the topographic surface and collect the seismic signals generated by a source located at the bottom of the aquifer to simulate a pumping system. First, cross-correlation of seismic traces with a reference one is used to produce interferograms (i.e., virtual surveys) for both the tested models. Then, direct P-wave arrivals identified in the two interferograms are compared through the stretching technique in order to estimate the relative velocity changes (dv/v). Finally, the estimated dv/v values are related to theoretical ones obtained using a reference subsurface model to produce the water level depth in the considered monitoring period.

Introduction

The analysis of the ambient seismic noise generated by both natural and artificial random sources has proved to be a useful tool to investigate the subsurface features for near-surface applications (Larose et al., 2015). Specifically, researchers have addressed the hydrogeological risks related to the activity of landslides (Taruselli et al., 2020a; Aguzzoli et al., 2021; Le Breton et al., 2021) and have monitored groundwater-level variations (Garambois et al., 2019; Taruselli et al., 2020b). Seismic noise, or passive, interferometry (SNI) is an effective tool for turning ambient vibrations into useful signals, i.e., retrieve the Green's function of the investigated media (Curtis et al., 2006). The technique relies on the cross-correlation of two noise recordings collected by sensors deployed at stable positions, and can provide new seismic responses by actually turning one of the receivers into a virtual source (Wapenaar et al., 2010). SNI requires that all sources be uncorrelated and homogenously spread around the considered receivers. SNI is particularly helpful for monitoring purposes because it allows detecting small differences between the seismic responses retrieved over time due to the variation of the subsurface features. This is the case, for instance, of water table-level changes that can alter seismic wave propagation into the subsurface. To this regard, researchers have resorted to coda wave interferometry (CWI), which uses multiply scattered waves in the investigated media around the considered receivers, to monitor subtle velocity variations of surface waves and track water-table oscillations (Mainsant et al., 2012; Voisin et al., 2016). The comparison between data obtained at different monitoring epochs is generally performed through the stretching technique (ST; Sens-Schönfelder and Wegler, 2006), that stretches or shrinks the monitoring cross-correlation to be as similar as possible to the reference one. The technique can be applied to data either in the frequency or in the time domain, and yields the stretching factor that, changed in sign, is the relative velocity variation occurred between the considered monitoring epochs because of groundwater-level changes. A previous work (Voisin et al., 2017) has shown that the estimation of water table-level variations with CWI is negatively affected by artificial sources as pumps activated discontinuously during the monitoring period. In fact, changing source characteristics is undesirable. However, by selecting only time spans in which pumps are active, it should be possible to detect velocity changes through the ST. In this work, we test whether the ST is reliable for monitoring the groundwater-level variations over time, even when applied to direct P-waves, by simulating a noise signal produced by an active pump. We consider noise signals collected during two modelling tests representing different monitoring periods, in which the water table of an unconfined aquifer was lowered and raised, respectively. Finally, the comparison between the direct P-waves velocity variation (dv/v) and the theoretical dv/v obtained from the reference model provides the water-level depth during the considered monitoring period.

Models

The modelling tests were carried out with the *Fdelmodc* software that relies on the finite-difference method to solve the 2D wave equation (Thorbecke and Draganov, 2011). The input models simulate seismic noise measurements in a lossless elastic medium during different monitoring periods, hereafter named M1 and M2 (Figures 1a and 1b), in which the water level of an unconfined aquifer is at 8 m and 10 m depth, respectively. Both models are 1000x200 m, have a 3-layer structure involving a top layer of dry soil (Vp = 1300 m/s, Vs = 500 m/s, ρ = 2000 kg/m^3), a middle layer representing saturated soil (Vp = 1500 m/s, Vs = 450 m/s, ρ = 2200 kg/m^3), and bedrock as the half-space starting at 20 m depth (Vp = 2000 m/s, Vs = 800 m/s, ρ = 2400 kg/m^3). A receiver spread of 33 sensors, placed along the topographic surface from 452 to 548 m (Figure 1), record the seismic noise for 20 s with a sampling interval of 0.001 s. The work focuses on receivers 1 and 17, which are the farthest from and nearest to the source, respectively. The source is placed at the midpoint of the x-axis and at 19 m depth close to the bottom of the aquifer to simulate the presence of a pumping system. It generates a noise signal 6 s long, with a frequency range between 30 and 40 Hz. The source is the same for both modelling tests as the seed number is kept constant and collected synthetic seismic traces are perturbed by adding white noise.
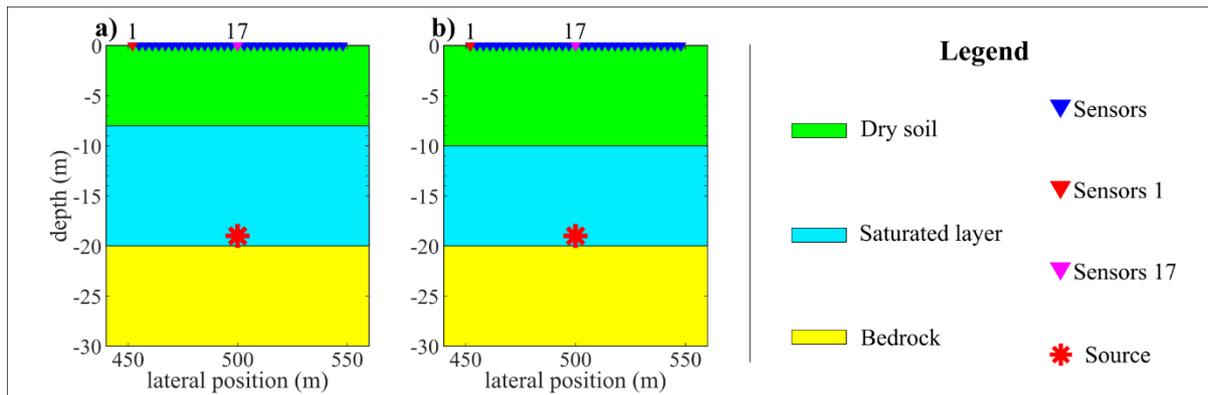
Figure 1: Zoomed sections of the models a) M1 b) and M2 used in the simulation performed with the Fdelmodc software; triangles are receivers and the star is the seismic noise source. See text for details.

Processing

The method relies on the idea that the water-level variation affects the velocity with which the P-waves propagate in the medium. Using SNI, we obtain a virtual survey with a virtual source at sensor 17 (Figure 1) by cross-correlating the trace recorded at sensor 17 with itself and all other traces. Figures 2a and 2b show the SNI results for models M1 and M2, respectively, that were high-pass filtered with a cut frequency of 1 Hz. Since the seismic interferometry effectively removes the travel path of waves that propagate from the real to the virtual source, the red circles in Figures 2a and 2b mark the arrival time of the P-wave that propagates from the real source to receiver 1 minus the time removed by the SNI. This difference changes according to the saturation of the subsurface. Figure 2c illustrates a section of the interferograms at sensor 1 for models M1 and M2 (hereafter I1 and I2, respectively) highlighting the peak of the direct P-wave arrival time. In the work presented here, we first apply the ST to several sub-windows of I1 that are stretched/shrunk in the frequency domain (Watson, 1986) to be as similar as possible to I2. Second, several sub-windows of I2 are stretched/shrunk to match I1. The theory of ST indicates that results derived from time windows with different lengths do not change if the value of the central time (CT) remains the same (Snieder, 2006). In our tests, the CT coincides with the arrival time of the P-wave that directly travels from the real source to sensor 1 minus the time removed by the SNI. The CT value can be calculated from the reference model (M1 in the first test and M2 in the second test), and changes depending on the initial saturation condition. Since we apply the ST in the frequency domain, using longer windows should improve the final results. On the other hand, the shorter the window, the lower the chances to include in the processing sequence interfering events that can produce an erroneous stretching factor. Thus, the window-length choice depends on the features of the case study and on the quality of the recordings; there is no possibility to define an optimal window length a priori. However, it is possible to define a range of values among which to choose the length of the window to increase the robustness of the final estimate. The maximum window should be less than 2CT, while the minimum length should be at least one period of the lowest frequency of interest. In Figure 2d, the amplitude spectra of I1 and I2 show a high peak in the same frequency band as the source (30-40 Hz). Thus, we use the lower limit of this band to define the minimum length of the window. The ST provides the ideal stretching factor that is the percentage value to apply to windows of I1 in order to obtain a signal as similar as possible to the corresponding window of I2. The inverse of the estimated stretching factor coincides with the dv/v occurring between the monitoring periods. By using the a priori information related to M1 when this model is the reference, i.e., water-level depth and P-wave velocity in both dry and saturated media, it is possible to obtain theoretical dv/v values as a function of the groundwater level. I.e., using Snell's law, we obtain the reference theoretical P-wave arrival time (T1) when the water table is at 8 m depth, as in M1. Then, we calculate another theoretical arrival time (T2) assuming that the water level changes over time reaching a depth of 10 m, as in M2. The relative time change between T1 and T2 coincides with the inverse of the theoretical dv/v. Modelled dv/v derived from the ST applied to I1 to match I2 should be equal to the theoretical dv/v value. In real-case studies, the water-level depth of a hypothetical monitoring period M2 is obviously unknown. However, we can calculate theoretical dv/v values starting from the a priori information of the initial subsurface model

M1 by varying the depth of the groundwater. The theoretical dv/v value closest to the estimated one indicates the depth of the water level in M2. In this work, when we stretch I1 we use the water level of M1 as a reference to calculate the theoretical dv/v, while the level of M2 is the reference when we stretch I2.
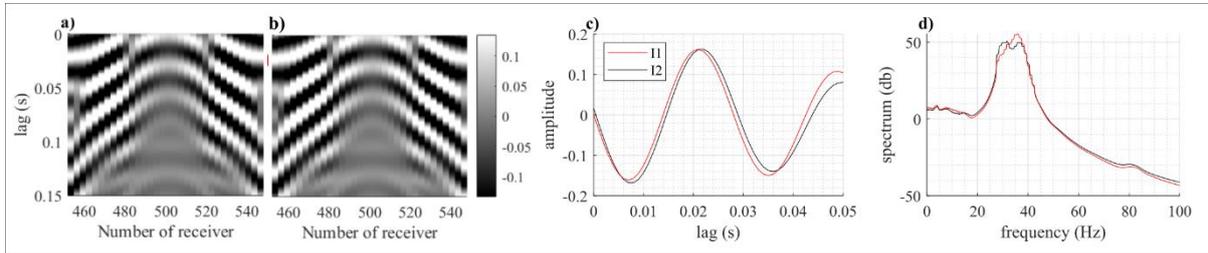

Figure 2: Result of the seismic interferometry for models a) M1 and b) M2. c) Interferograms at sensor 1 in a) and b) within the time window used to apply the ST. d) amplitude spectra for I1 and I2 in c). See text for details.

Results and discussion

Figures 3a and b show the comparison between the theoretical and the estimated dv/v values when M1 and M2 are used as references, respectively. Though for both tests perfect match is not achieved, the method provides a good estimate of the groundwater level. This means that the ST can also be applied to the direct P-waves. In more detail, in the first test the mean dv/v value computed over the time windows used to apply the ST is -2.3 % with a standard deviation of 0.4 (Figure 3a). Since dv/v values are negative, the velocity of P-waves propagating in M1 should decrease to match the one in M2. As far as groundwater depth is concerned, the computed dv/v values give a mean estimate of 11 m, while the actual depth is 10 m. In the second test, the mean dv/v value derived from stretching/shrinking I2 so as to match I1 is 1.1 % with a standard deviation of 0.1 (Figure 3b) indicating that the P-wave velocity in M1 is higher than in M2. The comparison between the estimated and theoretical dv/v values provides a mean water level of 8.2 m in M1, with longer windows indicating a water depth of 9 m, while shorter windows offer a perfect match of 8 m.
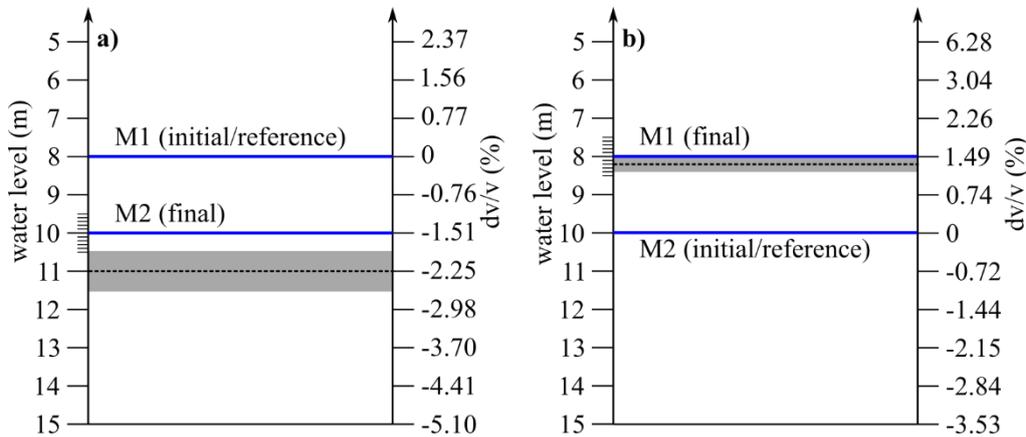

Figure 3: Results of dv/v estimation and of the associated water level depth considering a) M1 and b) M2 as the initial models. Dashed black line is the mean estimated value and grey shaded area is the standard deviation.

Conclusion

In this work we took into account two subsurface models representing the water-level variation of an unconfined aquifer where we generated synthetic seismic noise traces with a 2D finite-difference software. We processed modelled data with seismic noise interferometry followed by the stretching technique to retrieve water table depth changes. By comparing the estimated dv/v values to theoretical ones, we showed that we obtained a good estimate of the groundwater-level variation. Since our tests

involve only simple models, the method should be applied to more complex contexts and to data collected in field surveys. Overall, the technique appears very promising in monitoring the variation of the groundwater level over time by using the noise produced by a pumping system located inside the free aquifer.

References

Aguzzoli, A., Zanzi, L., and Arosio, D. [2021]. Seismic noise azimuthal spectral ratios to monitor landslide kinematics. Conference Proceedings, NSG2021 27th European Meeting of Environmental and Engineering Geophysics, Aug 2021, Volume 2021, p.1 – 5. DOI: https://doi.org/10.3997/2214-4609.202120213

Curtis, A., Gerstoft, P., Sato, H., Snieder, R., and Wapenaar, K. [2006]. Seismic interferometry—turning noise into signal. The Leading Edge, 25(9), 1082–1092. DOI: https://doi.org/10.1190/1.2349814

Garambois, S., Voisin, C., Romero Guzman, M. A., Brito, D., Guiller, B., and Réfloch, A. [2019]. Analysis of ballistic waves in seismic noise monitoring of water table variations in a water field site: added value from numerical modelling to data understanding. Geophysical Journal International, 219(3), 1636-1647. DOI: https://doi.org/10.1093/gji/ggz391

Larose, E., Carrière, S., Voisin, C., Bottelin, P., Baillet, L., Guéguen, P., Walter, F., Jongmans, D., Guillier, B., Garambois, S., Gimbert, F., and Massey, C. [2015]. Environmental seismology: What can we learn on earth surface processes with ambient noise? Journal of Applied Geophysics, 116, 62-74. DOI: http://dx.doi. org/10.1016/j.jappgeo.2015.02.001

Le Breton, M., Bontemps, N., Guillemot, A., Baillet, L., and Larose, E. [2021]. Landslide monitoring using seismic ambient noise correlation: challenges and applications. Earth-Science Reviews, 216, 103518. DOI: https://doi.org/10.10 16/j.ear scirev.2021.103518

Mainsant, G., Larose, E., Broennimann, C., Jongmans, D., Michoud, C., and Jaboyedoff, M. [2012]. Ambient seismic noise monitoring of a clay landslide: Toward failure prediction: Journal of Geophysical Research: Earth Surface, 117, F01030. DOI: https://doi.org/10.1029/2011JF002159

Sens-Schönfelder, C., and Wegler, U. C. [2006]. Passive image interferometry and seasonal variations of seismic velocities at Merapi Volcano, Indonesia. Geophys. Res. Lett. 33, L21302. DOI: 10.1029/2006GL027797

Snieder, R. [2006]. The Theory of Coda Wave Interferometry. Pure appl. geophys. 163, 455–473. DOI: https://doi.org/10.1007/s00024-005-0026-6

Taruselli, M., Aguzzoli, A., Zanzi, L. and Arosio, D. [2020a]. Monitoring Ca Lita Landslide by Means of the Ambient Seismic Noise. 3rd Asia Pacific Meeting on Near Surface Geoscience & Engineering, Conference Proceedings, 1-5. DOI: 10.3997/2214-4609.202071088.

Taruselli, M., Aguzzoli, A., Zanzi, L. and Arosio, D. [2020b]. Groundwater level monitoring tests with seismic interferometry. Conference Proceedings, NSG2020 26th European Meeting of Environmental and Engineering Geophysics, Dec 2020, Volume 2020, p.1 – 5. DOI: https://doi.org/10.3997/2214-4609.202020200

Thorbecke, J. W., and Draganov, D. [2011]. Finite-difference modeling experiments for seismic interferometry. Geophysics, 76(6), H1-H18. DOI: https://doi.org/10.1190/geo2010-0039.1

Voisin, C., Garambois, S., Massey, C., and Brossier, R. [2016]. Seismic noise monitoring of the water table in a deep-seated, slow-moving landslide. Interpretation, 4(3), SJ67–SJ76. DOI: https://doi.org/10.1190/INT-2016-0010.1

Voisin, C., Romero Guzmán, M.A., Réfloch, A., Taruselli, M. and Garambois, S. [2017]. Groundwater Monitoring with Passive Seismic Interferometry. Journal of Water Resource and Protection, 9, 1414-1427. DOI: https://doi.org/10.4236/jwarp.2017.912091

Wapenaar, K., Draganov, D., Snieder, R., Campman, X., and Verdel, A. [2010]. Tutorial on seismic interferometry: Part 1—Basic principles and applications. Geophysics, 75(5), 75A195-75A209. DOI: https://doi.org/10.1190/1.3457445

Watson, B., A. [1986]. Ideal shrinking and expansion of discrete sequences. NASA Technical Memorandum, 88202.